Geochemical evidence for a paired arc–back-arc association in the Neoarchean Gadwal greenstone belt, eastern Dharwar craton, India

Tarun C. Khanna*

National Geophysical Research Institute, Council of Scientific and Industrial Research, Hyderabad 500 007, India

Neoarchean Gadwal greenstone belt is situated in the eastern Dharwar craton, southern India. A well-preserved volcanic sequence which includes a boninite–adakite suite and normal tholeiitic to calc-alkaline basalt–andesite–dacite/rhyolite suite occurs in this belt. The focus of this study is the basaltic rocks from Gadwal greenstone belt. Based on their high field strength element and rare earth element (REE) data the basalts have been broadly grouped into two types: type I basalts are characterized by relatively high Nb/Th (5–9.2) and display slightly depleted to flat chondrite normalized REE patterns, whereas type II basalts display light-REE enriched patterns and Nb/Th ratio < 4. Both the types display uniform Nb/Y (~0.12) over a narrow range of Zr/Y (<3) ratios, and collectively exhibit negative Nb, Ti and minor Zr anomalies on a primitive mantle normalized trace element variation diagram. Alteration, metamorphism and contamination by assimilation of Archean upper continental crust in the study area can be ruled out as the cause of these anomalies. The incompatible trace element characteristics are consistent with a subduction related intraoceanic-arc setting for these volcanic rocks. The geochemical variations in Gadwal basalts cannot be explained by a two-stage mantle melting model as recently proposed for certain basalts from elsewhere (e.g. Pickle Crow Assemblage, Canada). The geochemical behaviour is attributed to the lateral variation and batch melting of a primitive mantle source involving subduction zone components. The Gadwal data together with recently published data on basaltic rocks from Archean and Phanerozoic subduction regimes have been used to suggest a Neoarchean paired arc–back-arc association in the eastern Dharwar craton.

Keywords: Archean, arc–back-arc, basalt, Gadwal greenstone belt, Dharwar craton.

TRACE elements, particularly the high field strength elements (HFSE; Nb, Zr, Th, Y) in conjunction with the rare earth elements (REEs) help in understanding the origin of volcanic rocks and constraining their geodynamic setting. Detailed geochemical studies of the volcanic rocks present in the various greenstone belts and also of granites adjacent to them in the Meso- to Neoarchean Dharwar craton of Peninsular India have indicated the occurrence of rare rock types and suggest operation of distinct magmatic processes at diverse tectonic settings[1–10]. The studies further suggest that the rocks were amalgamated in discreet tectonic terranes involving plume–arc interaction and accretion[5,8,11–13] which contributed to the growth and evolution of the Archean continental crust in the Dharwar craton[14].

High precision geochemical studies of the volcanic lithologies from the Archean granite–greenstone terranes in different cratonic provinces of the world indicated occurrence of subduction zone magmatic rocks[15–19], similar to the ones observed in the modern-day active intraoceanic arcs[20–23]. This essentially led to the suggestion that Phanerozoic style subduction zone magmatism was prevalent even during the Archean[19,24,25]. The objective of this study is to re-examine the existing geochemical data and present new chemical composition data for the metabasalts from Gadwal greenstone belt to show that: (i) they were formed in an intraoceanic-arc environment by subduction zone magmatism; (ii) the geochemical variations in Gadwal arc basalts cannot be accounted by two-stage melting of a mantle source and (iii) the geochemical signatures are consistent with a paired arc–back-arc association in the eastern Dharwar craton.

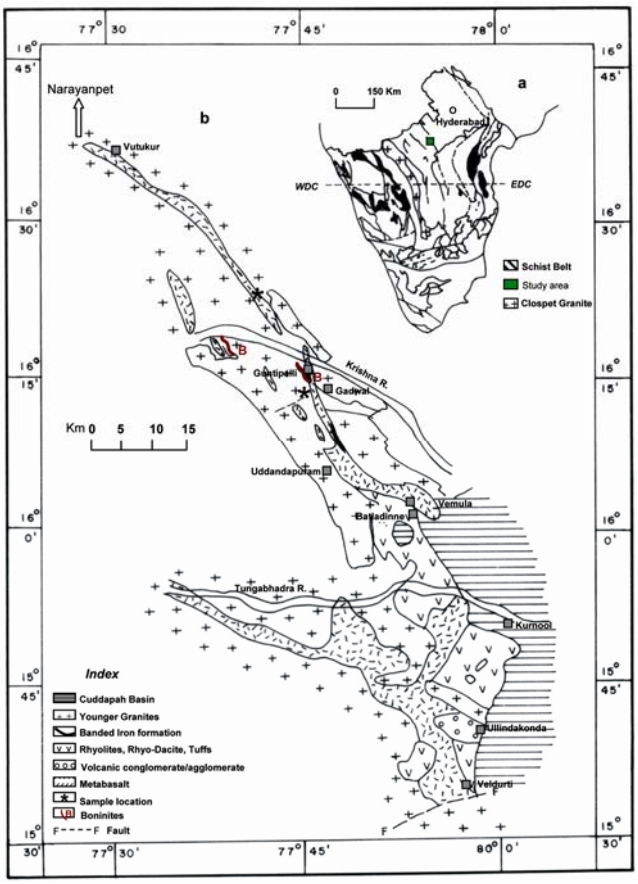

Figure 1. ***a***, Simplified geological map of southern peninsular India. ***b***, Generalized geological map of Gadwal greenstone belt[46].

*e-mail: khannangri@gmail.com

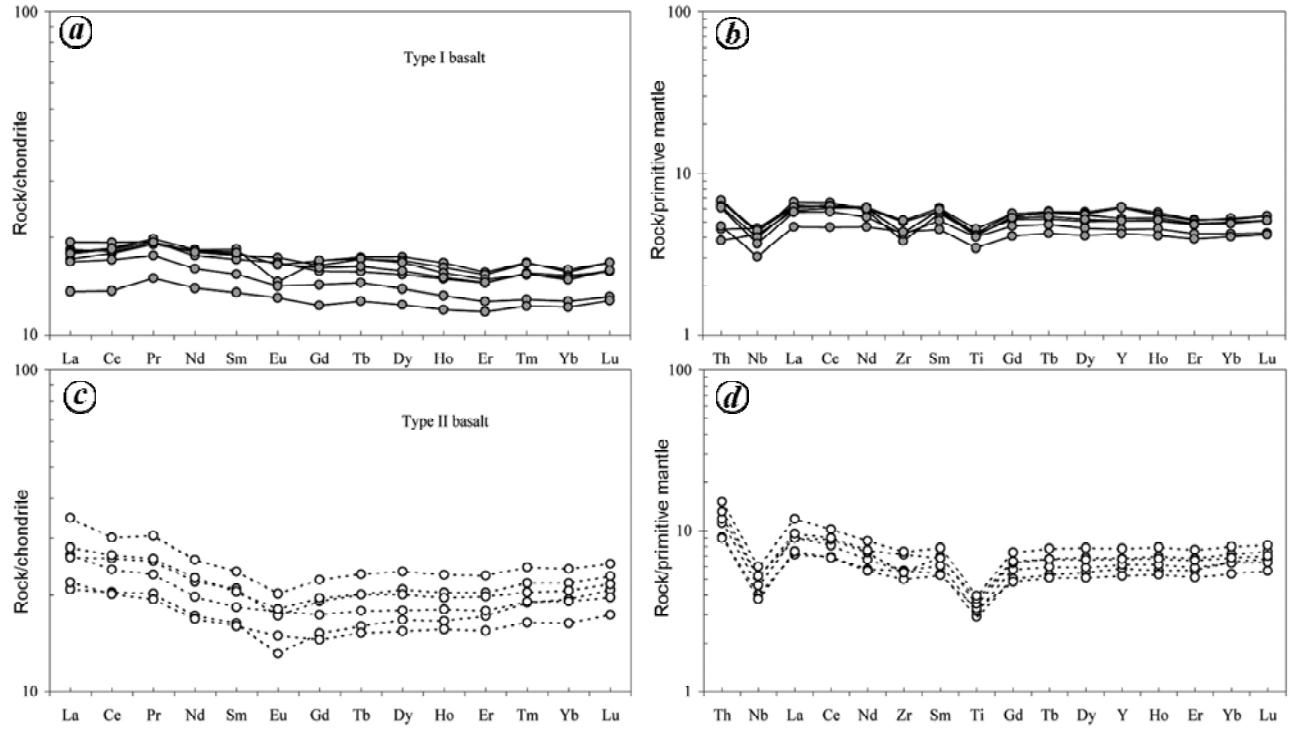

Figure 2. Chondrite normalized rare earth element (***a***, ***c***) and primitive mantle normalized trace element variation diagram (***b***, ***d***), for Gadwal basalts[34].

The Dharwar craton has been divided into eastern and western Dharwar blocks separated by a younger magmatic intrusion of linear trending ~2.6 Ga Closepet granite batholith (Figure 1 *a*). Studies suggest that the NNW–SSE trending shear zone, which extends all along the eastern margin of the Chitradurga greenstone belt, likely represents the boundary between the eastern and western blocks[4,26,27]. The Gadwal greenstone belt is situated in the eastern Dharwar craton. It extends from Narayanpet in the north to Veldurti in the south (Figure 1 *b*). The belt has a N–S trend in the southern part and NNW–SSE trend in the north, imparting an arcuate shape. The approximate strike length of the belt is ~90 km spanning over a variable width of 2–5 km. Three generations of folding have been recognized in this belt and the rocks have been metamorphosed to lower amphibolite facies[28]. The belt is surrounded by granites. Mafic dykes have been found to occur in the NE, east and SE parts of the belt. Some dikes trending N60°W extend to considerable lengths and exhibit cross-cutting relationship with the Gadwal belt. Neither the granites nor the dykes occurring in the vicinity of the Gadwal belt have been dated; however, recent work suggests a younger age of ~2.5 Ga for the granitoids in eastern Dharwar craton[4,29]. The combined Lu–Hf and Sm–Nd isotope studies yielded an age of ~2.70 Ga for the volcanic rocks of Gadwal greenstone belt[30].

Samples of volcanic rocks were selected from unsheared portions devoid of quartz veins or sulphide mineralization. Most of the samples display relict igneous textures, although metamorphosed to lower amphibolite facies. After petrographic screening, a subset of minimally altered samples has been selected for detailed geochemical studies. Rocks were powdered manually using an agate mortar. Analysis of ten major element oxides was performed on a Philips Magi XPRO PW2440, microprocessor-controlled, sequential XRF using pressed powder pellets. The relative standard deviations for the major element oxides were <3%. Minor and trace elements, including REE and HFSE, were determined by inductively coupled plasma mass spectrometry (ICP-MS, Perkin Elmer SCIEX ELAN DRC II). BHVO-1 and JB-2 were run as reference materials following the method described by Balaram and Gnaneswar Rao[31], and in concurrence with the recommended values of Govindaraju[32]; precision and accuracy in the analysed samples are better than 5% for majority of the trace elements. Chondrite[33] and primitive mantle[34] normalizations are indicated by subscript (N) and subscript (pm) respectively. Nb/Nb*, Zr/Zr* and Ti/Ti* ratios are calculated relative to the neighbouring REE[34].

In general, the volcanic rocks in the Archean granite–greenstone terranes are subjected to seafloor hydrothermal alteration, greenschist to amphibolite facies metamorphism and brittle–ductile deformation, which may cause certain elements to be mobile. Therefore, in keeping with the previous geochemical studies documented from the Archean terranes[17], the elements least susceptible to mobility and insensitive to the effects of alteration

Table 1. Major and trace element composition of metabasalts from Gadwal greenstone terrane, eastern Dharwar craton, India

	Type I							Type II					
	GWL-24[a]	GWL-26[a]	G-30[b]	G-31[b]	G-32[a]	G-36[b]	GWL-49[a]	G-49[b]	G-58[a]	G-53[b]	G-51[b]	G-50[b]	G-57[a]
SiO_2	51.85	52.25	51.23	51.51	51.05	51.38	52.00	51.77	53.71	53.79	54.19	54.76	55.42
TiO_2	0.92	0.89	0.91	0.98	0.90	0.87	0.75	0.69	0.52	0.71	0.77	0.82	0.86
Al_2O_3	13.08	13.09	13.86	15.23	14.00	13.03	13.12	12.93	13.71	13.62	14.05	13.98	13.35
Fe_2O_3	14.20	14.25	11.77	10.98	12.14	12.32	13.70	11.50	8.75	11.51	10.97	10.22	11.31
MnO	0.16	0.15	0.14	0.13	0.14	0.15	0.19	0.20	0.12	0.18	0.13	0.13	0.16
MgO	6.70	6.36	7.66	6.87	7.56	8.57	7.69	7.50	8.86	7.98	6.56	6.71	6.15
CaO	10.64	10.38	11.74	10.91	11.19	11.56	10.16	12.85	11.38	10.38	10.27	9.72	9.51
Na_2O	2.01	2.20	2.54	3.22	2.82	1.80	1.79	2.10	2.84	1.10	2.64	3.39	2.95
K_2O	0.32	0.30	0.05	0.07	0.09	0.25	0.54	0.35	0.04	0.64	0.30	0.14	0.14
P_2O_5	0.11	0.13	0.09	0.09	0.09	0.07	0.06	0.10	0.07	0.09	0.11	0.12	0.13
Mg#	48	47	56	55	55	58	53	56	67	58	54	57	52
Cr	151	137	209	245	199	184	166	17	109	41	11	16	11
Co	59	55	51	53	53	53	52	40	44	42	43	43	40
Ni	159	138	127	147	129	132	94	62	89	89	64	72	89
Rb	12	12	5	7	7	26	35	11	7	58	11	2	3
Sr	139	144	172	272	226	145	135	173	199	134	239	173	191
Cs	0.94	0.89	0.96	1.02	1.12	2.87	0.70	0.98	0.31	21.39	1.05	0.12	0.13
Ba	38	36	33	45	54	43	82	162	71	215	178	41	48
Sc	32	36	25	26	24	21	46	26	29	23	28	27	32
V	354	338	225	228	232	194	288	90	101	78	92	101	101
Nb	3.0	3.3	3.1	3.2	2.9	2.6	2.2	3.3	3.7	2.7	3.7	3.7	4.3
Zr	48	56	42	57	48	47	49	63	71	56	61	80	83
Hf	1.36	1.58	1.33	1.63	1.42	1.34	1.39	1.80	2.04	1.59	1.86	2.28	2.42
Th	0.32	0.38	0.57	0.58	0.53	0.52	0.40	0.95	1.09	0.76	1.01	1.12	1.29
U	0.12	0.14	0.26	0.23	0.23	0.17	0.12	0.33	0.34	0.25	0.32	0.33	0.34
Y	28	28	23	24	23	20	19	28	31	24	31	30	35
La	4.03	4.30	4.53	4.24	4.19	3.96	3.19	6.26	7.32	5.13	6.14	6.59	8.16
Ce	10.80	10.96	11.63	11.17	11.11	10.28	8.24	14.43	16.34	12.12	15.64	16.03	18.16
Pr	1.70	1.69	1.72	1.76	1.72	1.57	1.33	2.06	2.26	1.72	2.26	2.31	2.72
Nd	8.23	8.17	7.97	8.27	8.14	7.23	6.30	8.93	9.86	7.59	9.91	10.21	11.63
Sm	2.65	2.60	2.52	2.70	2.63	2.26	1.99	2.69	2.96	2.35	3.06	3.01	3.47
Eu	0.92	0.97	0.94	0.82	0.92	0.79	0.73	0.99	0.97	0.84	0.96	1.01	1.13
Gd	3.34	3.23	3.09	3.35	3.17	2.81	2.43	3.42	3.68	2.86	3.76	3.85	4.38
Tb	0.63	0.62	0.56	0.62	0.59	0.52	0.46	0.64	0.72	0.55	0.72	0.72	0.83
Dy	4.24	4.13	3.73	4.07	3.83	3.37	3.02	4.35	4.82	3.74	5.05	4.88	5.74
Ho	0.94	0.91	0.83	0.87	0.84	0.74	0.67	1.01	1.10	0.88	1.14	1.10	1.29
Er	2.48	2.44	2.30	2.36	2.31	2.02	1.88	2.83	3.17	2.46	3.23	3.15	3.65
Tm	0.40	0.40	0.37	0.37	0.37	0.31	0.30	0.46	0.51	0.39	0.52	0.49	0.58
Yb	2.55	2.59	2.48	2.45	2.41	2.07	1.99	3.11	3.41	2.66	3.54	3.36	3.92
Lu	0.40	0.40	0.38	0.38	0.38	0.32	0.31	0.47	0.52	0.42	0.55	0.52	0.60
Nb/Th	9.2	8.5	5.4	5.5	5.4	5.0	5.5	3.4	3.4	3.5	3.7	3.3	3.3
Nb/Nb[a]	0.88	0.86	0.65	0.68	0.65	0.61	0.65	0.45	0.45	0.46	0.51	0.46	0.45
Zr/Zr[a]	0.42	0.37	0.66	0.84	0.71	0.80	0.95	0.89	0.91	0.91	0.77	1.00	0.90
Ti/Ti[a]	0.74	0.73	0.77	0.77	0.74	0.82	0.80	0.54	0.37	0.65	0.54	0.57	0.52

[a]This study. [b]Data reported in Manikyamba and Khanna[41].

and metamorphism up to amphibolite facies, have been used to infer the primary, magmatic compositional characteristics of the Gadwal volcanic rocks. The Ce/Ce* ratio tightly clusters around 1.0 with a mean value of 0.98 in the basalts of present study, suggesting insignificant mobility of light-REE, during post-magmatic metamorphism and alteration[17]. Further, the relatively high Nb/Th (~9 versus 8 for primitive mantle[34]) coupled with mildly depleted to flat light-REE in some basalt samples of this study are inconsistent with crustal contamination, or assimilation and fractional crystallization of Archean upper continental crust[34] (discussed below). Moreover, the samples exhibit negative Nb, Zr and Ti anomalies consistent with a subduction-related origin and their formation in an oceanic-arc environment (discussed below; Figure 2).

The Gadwal basalts display uniform concentrations of MgO (~7.3 wt%), CaO (~10.8 wt%) and Al_2O_3 (~13.6 wt%), over a broad range of Mg# (47–67). Based on their trace element abundance, HFSE and REE characteristics, and inter-elemental ratios, these basalts have been broadly grouped into two types. The type I basalts consist

of relatively high TiO_2 (~0.9 wt%), Cr (~184 ppm) and Ni (~132 ppm), low Nb (~2.9 ppm), Zr (~50 ppm), Y (~24 ppm) and Th (~0.5 ppm) and variably high Nb/Th (5–9.2) ratios. They display slightly depleted to almost flat chondrite normalized REE (La_N/Sm_N = 0.9–1.1; Figure 2 *a*). On contrary, the type II basalts consist of low TiO_2 (~0.7 wt%), Cr (~34 ppm) and Ni (~77 ppm), comparatively high Nb (~3.6 ppm), Zr (~69 ppm), Y (~30 ppm) and Th (~1.04 ppm) and low Nb/Th (~3.5) ratios. They display light-REE enrichment $(La/Sm)_N \sim 1.4$, with a reversely fractionated heavy-REE $(Gd/Yb)_N < 1$ resembling U-shaped REE patterns (Figure 2 *c*). Collectively, both the groups display uniform Zr/Hf (~35) and Nb/Zr (~0.06) ratios, similar to the primitive mantle value of 36 and 0.06 respectively[12], and exhibit negative Nb, Zr and Ti anomalies on a primitive mantle normalized trace element variation diagram (Figure 2 *b* and *d*; Table 1).

The negative Nb anomalies are a characteristic feature of the rocks generated at convergent margin settings and also of the rocks derived from the upper continental crust. Contamination of the magma during their ascent by assimilation of crustal material, prior to their eruption onto the surface also results in negative Nb anomalies (e.g. continental flood basalts). Although there is compelling evidence for the prevalence of Archean upper continental crust in the eastern Dharwar craton[4,28,29], it is unlikely that the Gadwal basalts had either assimilated or interacted with this contemporaneous crustal material in the study area, due to the following reasons. (i) The absolute abundances of HFSE, REE and their inter-elemental ratios in the light-REE enriched basalts is significantly lower than that estimated for the Archean Upper Continental Crust[34] (Table A1 in Appendix 1), for example, Nb (~3.6 versus 13 ppm), Zr (~69 versus 125 ppm), Th (1.04 versus 5.7), La (~6.6 versus 20 ppm), Zr/Y (~2.3 versus 7), Nb/Y (~0.12 versus 0.72), Th/Y (~0.03 versus 0.32), Th/Ce (~0.07 versus 0.14), Th/Yb (0.31 versus 2.85), Zr/Sm (~23 versus 31), La/Sm (~2.26 versus 5), La/Yb (~1.98 versus 10) and Ce/Yb (~4.6 versus 21). (ii) The type I basalts exhibit normal mid-ocean ridge basalt (MORB)-like depleted REE patterns, coupled with similarly high Nb/Th (5–9) ratios, and overlap the fields defined by volcanic-arc basalts and normal MORB (discussed below). (iii) The mild light-REE enrichments in type II basalts are consistent, and overlap with the low Ce–Yb trend observed in modern-day intraoceanic-arc basalts[35] (Figure 3). (iv) Given the non-conservative behaviour of Rb, Sr, Ba, K, Th, U and light-REE (La, Ce, Nd) relative to the conservative behaviour of HFSE (Nb, Zr, Ti, Y) and heavy-REE (Gd, Dy, Yb) during slab dehydration and wedge melting processes[36], the progressive enrichment in light-REE and Th relative to heavy-REE, in concurrence with the magnitude of Nb anomalies, in the Gadwal basalts, essentially indicates flux-induced partial melting of the mantle wedge from subducted slab-derived fluids enriched in incompatible trace elements (Figure 4).

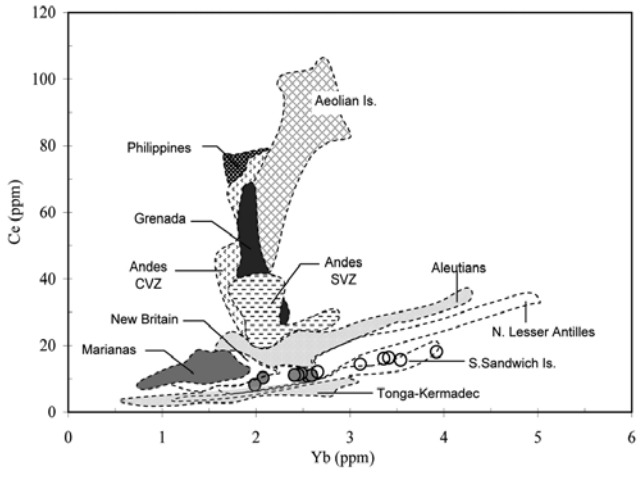

Figure 3. Yb versus Ce diagram in which the Gadwal basalts collectively plot in the modern-day active intraoceanic-arc basalt fields with consistently low Ce/Yb (~4.5) trend (after Hawkesworth *et al.*[35]).

Continental-arc basalts are generated by the subduction of an oceanic crust beneath a continental lithosphere (e.g. South Volcanic Zone–Andes). Though continental margin setting has been proposed for a few greenstone belts in the Dharwar craton[24,37] in contrast to intraoceanic-arc basalts, the continental-arc basalts are typically characterized by high Zr/Y (>3)[38] and Ti/Y (>400)[39] ratios. The Gadwal basalts collectively plot in the ocean basalt fields defined by normal MORB and volcanic arc basalts, and distinctly away from within-plate or continental tholeiites, in the Zr–Nb–Y space[40] (Figure 5). The relatively flat, primitive mantle normalized heavy-REE, and slightly higher range of Nb contents in Gadwal type I basalts (2.2–3.3) is comparable to the abundances in normal MORB (2.33)[34] and Archean depleted MORB-like melts (1.07–3.26)[18]. However, the average Nb/Th = 6.1, Nb/La = 0.7, Zr/Sm = 20 and Ti/Sm = 2151 ratios in type I basalts is much lower than that observed in normal MORB[34] (19, 0.9, 28 and 2890 respectively) and consequently, the negative Nb, Zr and Ti anomalies in Gadwal basalts are unlike those observed in MORB (Figure 6). Moreover, MORBs are high-degree partial melts formed at shallow depth in the upper mantle regions, and brought onto the surface of the ocean floor by the induced upwelling of the convecting mantle at spreading centres. Therefore, it is less likely that Gadwal type I basalts qualify as MORBs. Nevertheless, in addition to the above discussed geochemical characteristics, the collective occurrence of boninites, adakites, tholeiitic pillowed basalts and banded iron formations in the same belt, endorses an intraoceanic-arc setting for the Gadwal volcanic rocks[41].

Recently, a two-stage melting model for the Archean upper mantle was proposed for the generation of tholeiitic arc basalts in Neoarchean Pickle Crow Assemblage, Ontario, Canada[42]. According to this model, the basalts with

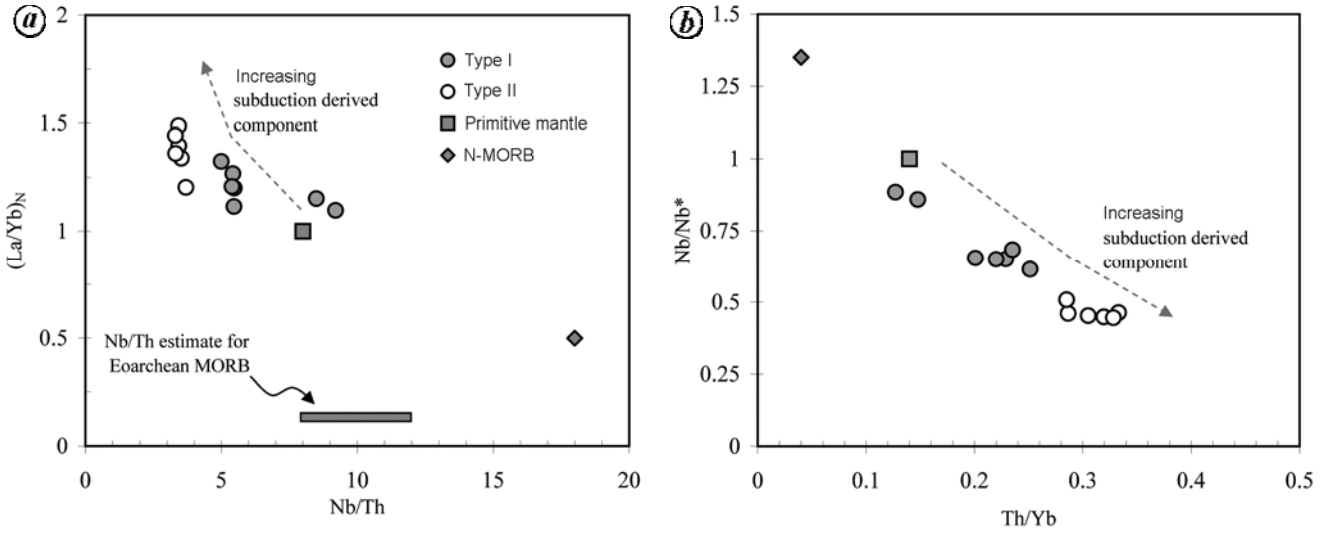

Figure 4. Ratio–ratio bi-variate plot of high field strength and rare earth elements for Gadwal basalts. Data sources for Eoarchean MORB[47], N-MORB[34] and primitive mantle[34] have been plotted for reference.

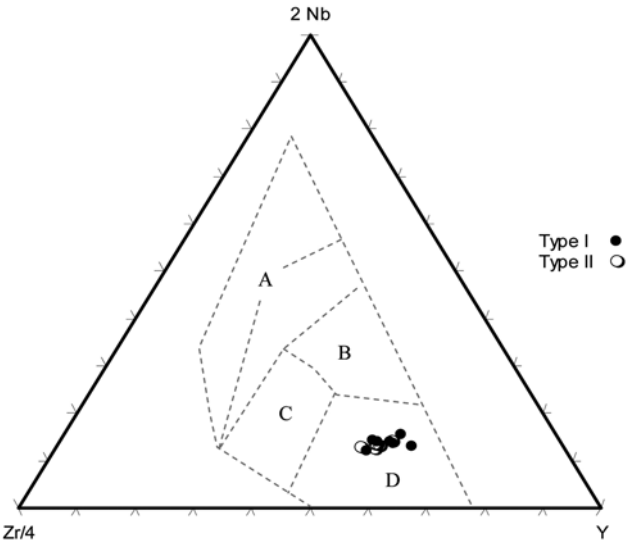

Figure 5. Zr–Nb–Y triangular discrimination diagram for Gadwal basalts (after Meschede[40]). The fields represent: A – Within-plate alkali basalts and within-plate tholeiites; B – E-type MORB; C – Within-plate tholeiites and volcanic-arc basalts and D – N-type MORB and volcanic-arc basalts.

negative Nb, P, Zr and Hf anomalies represent the first-stage melts, wherein the enrichments in light-REE and large ion lithophile elements (LILE) relative to HFSE are inherited from the subduction-derived component. After this prior extraction event, the residual mantle is compositionally impoverished in LREE relative to HFSE. The second-stage melts inherit these HFSE enrichments from the mantle and give rise to basalts with positive Nb/LREE and Hf/MREE (middle-REE). At first approximation, if it is taken that the Gadwal type II basalts with enriched LREE (Figure 2 *c*) represent the first-stage melts, then the LREE depleted arc basalts must inherit the positive Nb and Zr anomalies from the residual mantle, as expected in the case of second-stage melts. On the contrary, the Gadwal type I basalts are typically characterized by low $(Nb/La)_{pm}$ (~0.68) and $(Zr/Sm)_{pm}$ (~0.80) ratios. Therefore, it is unlikely that the geochemical variations in Gadwal arc basalts represent the melt products of multiple extraction events. Rather, the geochemical signatures in Gadwal basalts are attributed to lateral variations and variable degrees of partial melting of a primitive mantle source (see Figure A1 in Appendix 1) involving subduction zone components (discussed below).

Fryer *et al.*[43] were the first to use the term 'back-arc basin basalts' which display geochemical characteristics transitory between normal MORB and island arc basalts. Pearce and Stern[44] made a comprehensive study of the rocks generated in the modern-day arc/back-arc regions from Izu-Bonin, Lau-Tonga, Marianas, Scotia, Manus and noted that the back-arc basalts are compositionally characterized by enrichments in non-conservative elements and depletions in conservative elements, which are strongly controlled by the addition of subduction-derived fluids in their mantle source regions. Further, they also showed that the trace elements having similar partition coefficients during mantle melting and crystallization processes can readily indicate the magnitude of mantle fertility in these volcanics relative to a normal MORB source. Therefore, given the moderately incompatible behaviour and least susceptibility to mobility during subduction zone magmatic processes, Nb, Yb abundances and Nb/Yb ratio have been used as fractionation-independent proxy to asses the mantle input and conditions of partial melting in the arc/back-arc regions. Mobility of Ba, Th and light-REE in the subduction fluids increases with increase in temperature. Therefore Ba/Th,

Ba/Nb, Th/Nb and La/Nb ratios are effectively used to trace the magnitude of subduction input. Further, the magnitude of subduction input in the back-arc regions is laterally proportional to its distance from the arc, such that the rocks generated proximal to the arc display high Ba/Nb, Th/Nb and La/Nb compared to those generated distal to the arc[44].

As a corollary, the average abundances of Gadwal type I and type II basalts plotted in Figure 6 *c*, and normalized to normal MORB[34], collectively display strong enrichments in Ba, Th, La, Ce and mildly enriched Nb relative to normal MORB. When compared to the type II basalts, the type I basalts are characterized by low Ba/Nb, Th/Nb, La/Nb, and similarly high Nb/Yb ratios. This suggests that the type I basalts were apparently generated by the partial melting of a mantle source fluxed with lower magnitude of subduction input and relatively distal to the arc, whereas the type II basalts with similar Nb content and Nb/Yb ratio were generated from the same mantle wedge, at a shallow depth involving high subduction input and proximal to the arc.

In the Zr–Nb–Y tectonic discrimination diagram[40] (Figure 5), the Gadwal arc basalts collectively plot in the ocean basalt field defined by normal MORB and volcanic arc basalts. To discriminate further and better constrain the tectonic setting, the Gadwal basalts were plotted in a La–Y–Nb triangular plot[45], wherein the type II basalts straddle the boundary between volcanic arc basalts and back-arc basalts, and the type I basalts distinctively plot in the back-arc basalt field (Figure 7). This geochemical behaviour is also apparent in the TiO_2 versus $(La/Sm)_N$ discrimination diagram (Figure 8 *a*), and in Nb/Yb versus Th/Yb coordinate space (Figure 8 *b*), in which the type II basalts with enriched light-REE and Th, plot in the Phanerozoic arc basalt field and the type I basalts plot in the Phanerozoic back-arc fields, transitory to normal MORB and island arc basalts. These geochemical characteristics are also consistent with Neoarchean basalts, published in the literature (Figure 8 *c*), that are inferred to be generated in intraoceanic-arc settings representing paired arc–back-arc association. Besides, the occurrence of boninites and adakites in Gadwal greenstone belt, the HFSE and REE systematics observed in the light-REE enriched and

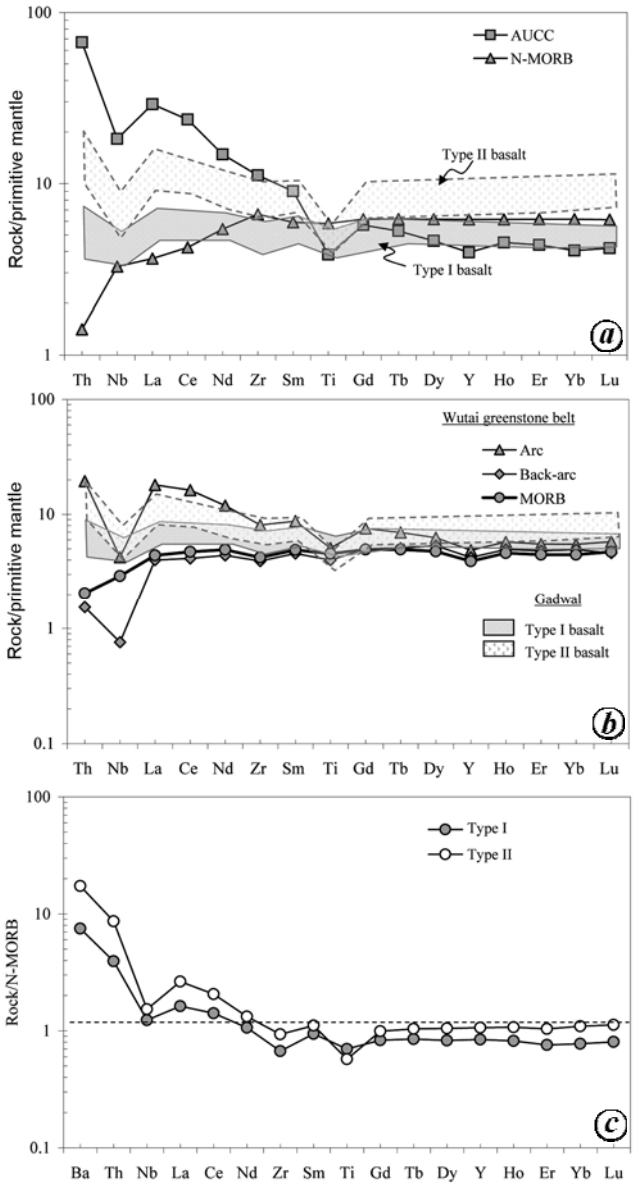

Figure 6. Primitive mantle normalized trace element variation diagram for: ***a***, Archean upper continental crust (AUCC) and normal mid-ocean ridge basalt (N-MORB)[34]; ***b***, NeoArchean arc, back-arc and MORB are plotted from Wutai greenstone belt, North China Craton[18], for comparison with the sample field envelope of Gadwal type I and type II basalts, shown as shaded regions. ***c***, N-MORB normalized incompatible trace element variation diagram for Gadwal basalts[34]. Data plotted are the average of type I and type II, given in Table A1 (Appendix 1).

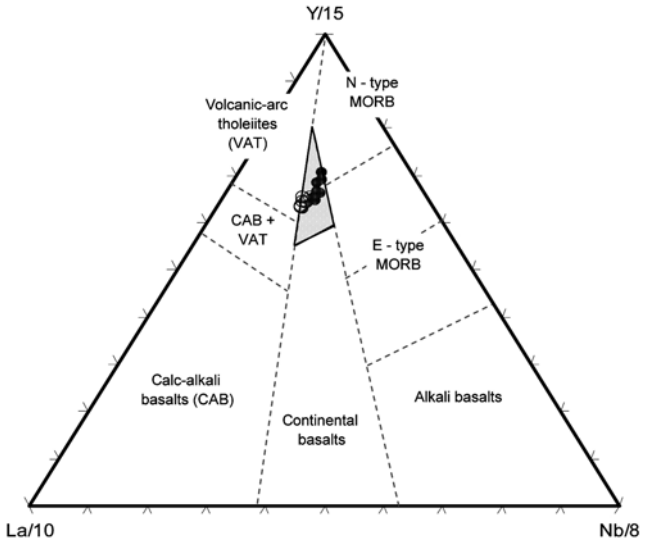

Figure 7. La–Y–Nb triangular discrimination diagram for Gadwal basalts, in which the type II basalts straddle the boundary between volcanic-arc basalts and back-arc basalts, while the type I basalts distinctly plot in the narrow field defined by back-arc basalts (after Cabanis and Lecolle[45]).

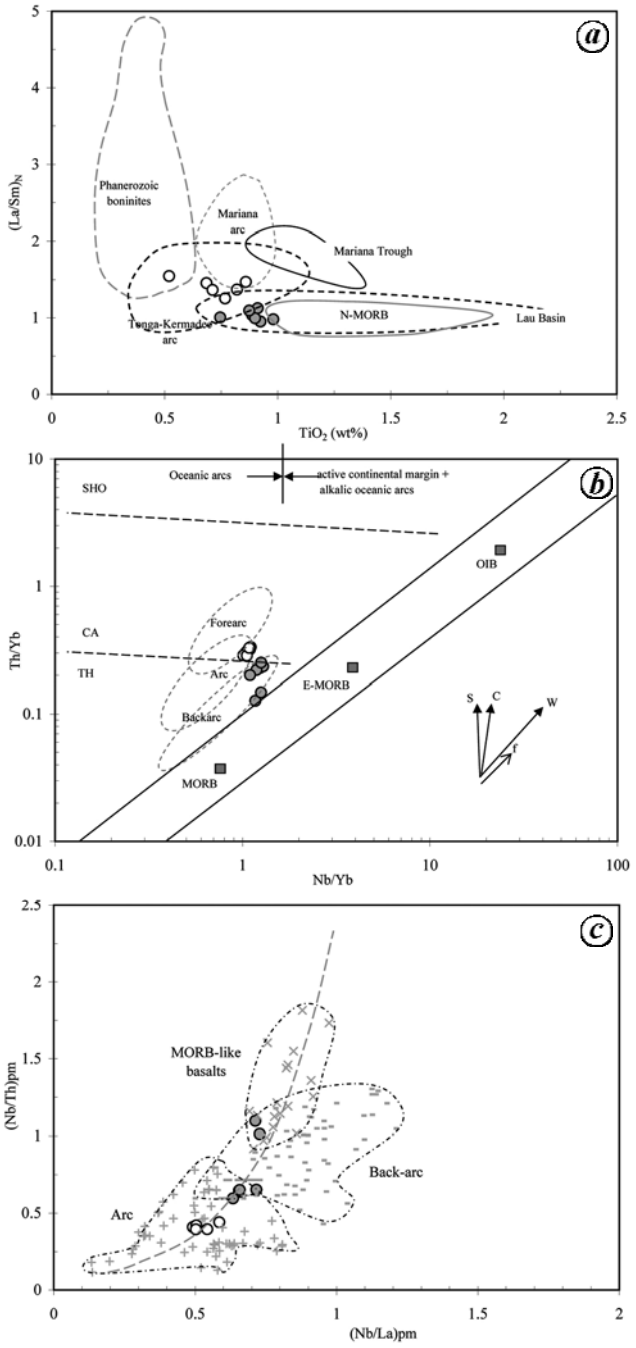

Figure 8. ***a***, $(La/Sm)_N$ versus TiO_2 discrimination plot for Gadwal basalts in which type I occupies the modern-day back-arc fields, and type II plots distinctly in the moden arc fields[48]. ***b***, Nb/Yb versus Th/Yb discrimination diagram[49] in which the Gadwal basalts trend sub-parallel and oblique to the modern MORB-OIB array, and occupy the Phanerozoic arc–back-arc fields[50]. ***c***, Primitive mantle normalized Nb/La versus Nb/Th diagram for Gadwal arc basalts[34]. The fields for Archean basaltic rocks have been compiled from the GEOROCK (http://georoc.mpch-mainz.gwdg.de) database.

depleted arc basalts endorse Phanerozoic-style subduction zone magmatism in the eastern Dharwar craton.

The geochemical characteristics of arc basalts, and the occurrence of boninites, adakites, tholeiitic pillowed basalts and banded iron formations endorse an intra-oceanic-arc setting for the Gadwal greenstone belt. The geochemical variations in Gadwal arc basalts do not represent the melt products of multiple extraction events. Instead, they are attributed to lateral variations and various degrees of partial melting of a primitive mantle source involving subduction zone components.

Based on the geochemical evidence presented in this communication, it is proposed that the Gadwal basalts represent a Neoarchean paired arc–back-arc sequence in the eastern Dharwar craton.

The light-REE enriched and depleted arc basalts associated with boninites and adakitic rocks in the Gadwal belt, combined with the geochemical characteristics of the arc basalts from other Neoarchean terranes, contribute to better understanding that the Phanerozoic-style subduction zone magmatic processes existed during the Neoarchean.

Appendix 1

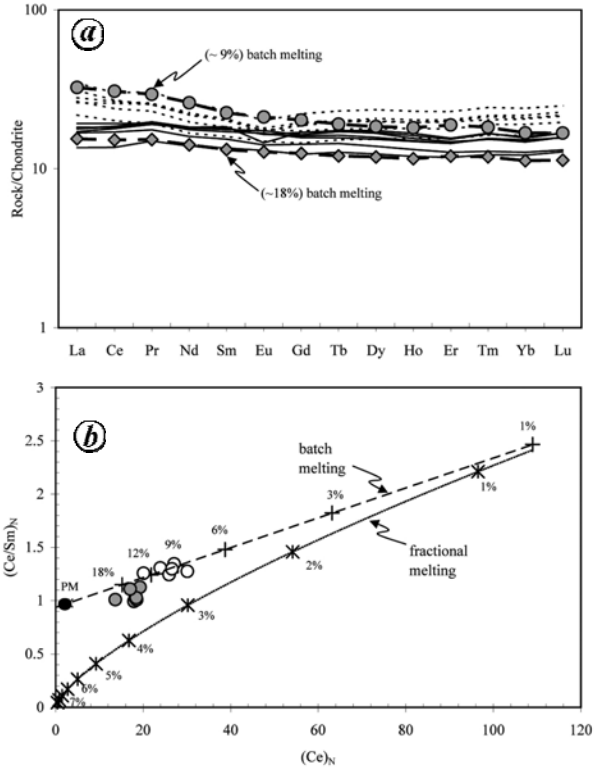

Figure A1. ***a***, About 18% and ~9% batch melting of a primitive mantle source in the spinel–lehrzolite stability field can demonstrably explain the subtle geochemical variations in the light rare earth element systematics of type I (solid lines) and type II (dotted lines) basalts respectively, in Gadwal greenstone belt. ***b***, Various percentile batch and fractional melting curves calculated from the equations in Rollinson[51], with the same source mineralogy have been plotted for comparison. Symbols are same as in Figure 2. It is apparent that fractional melting cannot explain the geochemical variations observed in the Gadwal basalts. Source mineralogy (Ol = 0.53, Opx = 0.24, Cpx = 0.20, and Sp = 0.03), and melting proportions (Ol = –0.30, Opx = 0.40, Cpx = 0.82 and Sp = 0.08) have been adopted from Gurenko and Chaussidon[52]; partition coefficient data are from McKenzie and O'Nions[53] and Shaw[54]; as summarized in Vijay Kumar *et al.*[55]. Primitive mantle and chondrite normalization values are from Sun and McDonough[33].

Table A1. Representative trace element concentrations from distinct tectonic settings

	AUCC[a]	N-MORB[b]	Arc[c]	Back-arc[c]	MORB[c]	Arc[d]	Back-arc[d]
Ti	5000	7600	6600	5186	5887	4358	5328
Nb	13	2.33	3.02	0.54	2.07	3.56	2.87
Zr	125	74	90	44	47	69	50
Th	5.7	0.12	1.65	0.13	0.17	1.04	0.47
Y	18	28	22	19	18	30	24
La	20.00	2.50	12.38	2.75	3.02	6.60	4.06
Ce	42.00	7.50	28.76	7.34	8.38	15.45	10.60
Pr	4.90	1.32	3.78	1.15	1.32	2.22	1.64
Nd	20.00	7.30	16.02	5.93	6.65	9.69	7.76
Sm	4.00	2.63	3.87	2.03	2.17	2.92	2.48
Eu	1.20	1.02	1.16	0.74	0.75	0.98	0.87
Gd	3.40	3.68	4.48	2.97	2.95	3.66	3.06
Tb	0.57	0.67	0.75	0.55	0.53	0.70	0.57
Dy	3.40	4.55	4.61	3.93	3.51	4.76	3.77
Ho	0.74	1.01	0.94	0.81	0.75	1.09	0.83
Er	2.10	2.97	2.64	2.30	2.13	3.08	2.25
Tm	0.30	0.46	0.40	0.36	0.33	0.49	0.36
Yb	2.00	3.05	2.70	2.43	2.20	3.33	2.36
Lu	0.31	0.46	0.43	0.34	0.35	0.51	0.37

Data source: [a]Taylor and McLennan[34]; [b]Sun and McDonough[33]; [c]Average compositions from Wang *et al*.[18]; [d]This study.

1. Rajamani, V., Shivkumar, K., Hanson, G. N. and Shirey, S. B., Geochemistry and petrogenesis of amphibolites from the Kolar Schist Belt, South India: evidence for ultramafic magma generation by low percent melting. *J. Petrol.*, 1985, **26**, 92–123.
2. Rajamani, V., Shirey, S. B. and Hanson, G. N., Fe-rich Archean tholeiites derived from melt-enriched mantle sources: evidence from the Kolar Schist Belt, South India. *J. Geol.*, 1989, **97**, 487–501.
3. Balakrishnan, S., Hanson, G. N. and Rajamani, V., Pb and Nd isotope constraints on the origin of high Mg and tholeiitic amphibolites Kolar Schist Belt, South India. *Contrib. Mineral. Petrol.* 1990, **107**, 279–292.
4. Jayananda, M., Moyen, J-F., Martin, H., Peucat, J.-J., Auvray, B. and Mahabaleshwar, B., Late Archaean (2550–2520 Ma) juvenile magmatism in the eastern Dharwar craton, southern India: constraints from geochronology, Nd–Sr isotopes and whole rock geochemistry. *Precambrian Res.*, 2000, **99**, 225–254.
5. Jayananda, M., Kano, T., Peucat, J. J. and Channabasappa, S., 3.35 Ga komatiite volcanism in the western Dharwar craton, southern India: 16 constraints from Nd isotopes and whole-rock geochemistry. *Precambrian Res.*, 2008, **162**, 160–179.
6. Manikyamba, C., Naqvi, S. M., Subba Rao, D. V., Ram Mohan, M., Khanna, T. C., Rao, T. G. and Reddy, G. L. N., Boninites from the Neoarchaean Gadwal greenstone belt, eastern Dharwar craton, India: implications for Archaean subduction processes. *Earth Planet. Sci. Lett.*, 2005, **230**, 65–83.
7. Manikyamba, C., Kerrich, R., Khanna, T. C. and Subba Rao, D. V., Geochemistry of adakites and rhyolites from the Neoarchean Gadwal greentsone belt, eastern Dharwar craton, India. Implications for sources and geodynamic setting. *Can. J. Earth Sci.*, 2007, **44**, 1517–1535.
8. Manikyamba, C., Kerrich, R., Khanna, T. C., Krishna, A. K. and Satyanarayanan, M., Geochemical systematics of komatiite–tholeiite and adakite–arc basalt associations: the role of a mantle plume and convergent margin in formation of the Sandur Superterrane, Dharwar craton. *Lithos*, 2008, **106**, 155–172.
9. Manikyamba, C., Kerrich, R., Khanna, T. C., Satyanarayanan, M. and Krishna, A. K., Enriched and depleted arc basalts, with high-Mg andesites and adakites: a potential paired arc–backarc of the 2.7 Ga Hutti greenstone terrane, India. *Geochim. Cosmochim. Acta*, 2009, **73**, 1711–1736.
10. Naqvi, S. M., Khan, R. M. K., Manikyamba, C., Ram Mohan, M. and Khanna, T. C., Geochemistry of the Neoarchaean high-Mg basalts, boninites and adakites from the Kushtagi–Hungund greenstone belt of the eastern Dhawar craton (EDC); implications for the tectonic setting. *J. Asian Earth Sci.*, 2006, **27**, 25–44.
11. Chadwick, B., Vasudev, V. N. and Ahmed, N., The Sandur schist belt and its adjacent plutonic rocks: implications for late Archaean crustal evolution in Karnataka. *J. Geol. Soc. India*, 1996, **47**, 37–57.
12. Chadwick, B., Vasudev, V. N. and Hegde, G. V., The Dharwar craton, southern India, interpreted as the result of late Archaean oblique convergence. *Precambrian Res.*, 2000, **99**, 91–111.
13. Balakrishnan, S., Rajamani, V. and Hanson, G. N., U–Pb ages for zircon and titanite from the Ramagiri area, southern India: evidence for the accretionary origin of the eastern Dharwar craton during the late Archean. *J. Geol.*, 1999, **107**, 69–86.
14. Naqvi, S. M. and Rogers, J. J. W., *Precambrian Geology of India*, Oxford University Press, New York, 1987, p. 223.
15. Wyman, D. A., Ayer, J. A. and Devaney, J. R., Niobium-enriched basalts from the Wabigoon subprovince, Canada: evidence for adakitic metasomatism above an Archaean subduction zone. *Earth Planet. Sci. Lett.*, 2000, **179**, 21–30.
16. Polat, A. and Kerrich, R., Magnesian andesites, Nb-enriched basalt–andesites, and adakites from late Archean 2.7 Ga Wawa greenstone belts, Superior Province, Canada: implications for late Archean subduction zone petrogenetic processes. *Contrib. Mineral. Petrol.*, 2001, **141**, 36–52.
17. Polat, A., Hofmann, A. W. and Rosing, M. T., Boninite-like volcanic rocks in the 3.7–3.8 Ga Isua greenstone belt, West Greensland: geochemical evidence for intra-oceanic subduction zone processes in the early Earth. *Chem. Geol.*, 2002, **184**, 231–254.
18. Wang, Z., Wilde, S. A., Wang, K. and Yu, L., A MORB-arc basalt–adakite association in the 2.5 Ga Wutai greenstone belt: Late Archean magmatism and crust growth in the North China Craton. *Precambrian Res.*, 2004, **131**, 323–342.
19. Smithies, R. H., Champion, D. C., Van Kranendonk, M. J., Howard, H. M. and Hickman, A. H., Modern-style subduction processes in the Mesoarchaean: geochemical evidence from the 3.12 Ga Whundo intra-oceanic arc. *Earth Planet. Sci. Lett.*, 2005, **231**, 221–237.
20. Pearce, J. A., van der Laan, S. R., Arculus, R. J., Murton, B. J., Ishii, T., Peate, D. W. and Parkinson, I. J., Boninite and harzburgite from Leg 125 (Bonin–Mariana forearc): a case study of magma genesis during the initial stages of subduction. In Proceedings of the Ocean Drilling Program, Scientific Results, Ocean Drilling Program 125, College Station, Texas, 1992, pp. 623–659.
21. Yogodzinski, G. M., Kay, R. W., Volynets, O. N., Koloskov, A. V. and Kay, S. M., Magnesian andesites in the western Aleutian Komandorsky region: implications for slab melting processes in the mantle wedge. *Geol. Soc. Am. Bull.*, 1995, **107**, 505–519.
22. Drummond, M. S., Defant, M. J. and Kepezhinskas, P. K., Petrogenesis of slab-derived trondhjemite-tonalite-dacite/adakite magmas. *Trans. R. Soc. Edinburgh, Earth Sci.*, 1996, **87**, 205–215.
23. Sajona, F. G., Maury, R. C., Bellon, H., Cotton, J. and Defant, A. M., High field strength element enrichment of Pliocene–Pleistocene Island arc basalts, Zamboanga Peninsula, Western Mindanao (Philippines). *J. Petrol.*, 1996, **37**, 693–726.
24. Krogstad, E. J., Hanson, G. N. and Rajamani, V., Sources of continental magmatism adjacent to the late Archean Kolar Suture Zone, South India: distinct isotopic and elemental signatures of two late Archean magmatic series. *Contrib. Mineral. Petrol.*, 1995, **122**, 159–173.

25. Polat, A. and Kerrich, R., Reading the geochemical fingerprints of Archean hot subduction volcanic rocks: evidence for accretion and crustal recycling in a mobile tectonic regime. *Am. Geophys. Monogr*., 2006, **164**, 189–213.
26. Swami Nath, J., Ramakrishnan, M. and Viswanatha, M. N., Dharwar stratigraphic model and Karnataka craton evolution. *Rec. Geol. Surv. India*, 1976, **107**, 149–175.
27. Naqvi, S. M., Chitradurga schist belt – an Archaean suture(?). *J. Geol. Soc. India*, 1985, **26**, 511–525.
28. Matin, A., Structure of the Gadwal schist belt, eastern Dharwar craton, Mahbubnagar and Kurnool District, Andhra Pradesh. *Indian J. Geol.*, 2001, **73**, 199–205.
29. Moyen, J. F., Martin, H., Jayananda, M. and Auvray, B., Late Archaean granite: a typology based on the Dharwar craton (India). *Precambrian Res*., 2003, **127**, 103–123.
30. Khanna, T. C., Bizimis, M., Yogodzinski, G. M. and Balaram, V., Lutetium–hafnium isotopic systematics of the metavolcanic rocks from 2.70 Ga Gadwal greenstone terrane, Dharwar craton, India: implications for the evolution of the Eoarchean mantle. In 34th International Geological Congress, Brisbane, Australia, 2012.
31. Balaram, V. and Gnaneswar Rao, T., Rapid determination of REE and other trace elements in geological samples by microwave acid digestion and ICPMS. *At. Spectrosc*., 2003, **24**, 206–212.
32. Govindaraju, K., Compilation of working values and sample description for 33 Geostandards. *Geostand. Newsl.* (*Spec. Issue*), 1994, **18**, 158.
33. Sun, S.-S. and McDonough, W. F., Chemical and isotopic systematics of oceanic basalts: implications for mantle compositions and processes. In *Magmatism in Ocean Basins* (eds Saunders, A. D. and Norry, M. J.), Geological Society of London, 1989, vol. 42, pp. 313–345.
34. Taylor, S. R. and McLennan, S. M., *The Continental Crust: Its Composition and Evolution*, Blackwell, Oxford, 1985, p. 312.
35. Hawkesworth, C. J., McDermott, F., Peate, D. W. and van Calsteren, P., Mantle and slab contributions in arc magmas. *Annu. Rev. Earth Planet. Sci*., 1993, **21**, 175–204.
36. Pearce, J. A., Stern, R. J., Bloomer, S. H. and Fryer, P., Geochemical mapping of the Mariana arc–basin system: implications for the nature and distribution of subduction components. *Geochem. Geophys. Geosyst*., 2005, **6**, Q07006, doi:10.1029/2004GC000895.
37. Naqvi, S. M. and Rana Prathap, J. G., Geochemistry of adakites from Neo-Archaean active continental margin of Shimoga schist belt, western Dharwar craton, India: implications for the genesis of TTG. *Precambrian Res*., 1987, **156**, 32–54.
38. Pearce, J. A. and Norry, M. J., Petrogenetic implications of Ti, Zr, Y and Nb variations in volcanic rocks. *Contrib. Mineral. Petrol*., 1979, **69**, 33–47.
39. Pearce, J. A., Trace element characteristics of lavas from destructive plate boundaries. In *Andesites* (ed. Thorpe, R. S.), Wiley, 1982, pp. 525–548.
40. Meschede, M., A method of discriminating between different types of midocean ridge basalts and continental tholeiites with the Nb–Zr–Y diagram. *Chem. Geol*., 1986, **56**, 207–218.
41. Manikyamba, C. and Khanna, T. C., Crustal growth processes as illustrated by the Neoarchean intraoceanic magmatism from Gadwal greenstone belt, eastern Dharwar craton, India. *Gondwana Res.*, 2007, **11**, 476–491.
42. Hollings, P. and Kerrich, R., Geochemical systematics of tholeiites from the 2.86 Ga Pickle Crow Assemblage, northwestern Ontario: arc basalts with positive and negative Nb–Hf anomalies. *Precambrian Res*., 2004, **134**, 1–20.
43. Fryer, P., Sinton, J. M. and Philpotts, J. A., Basaltic glasses from the Mariana Trough. In *Initial Reports of the Deep Sea Drilling Project, 60* (eds Hussong, D. M. *et al*.), US Government Printing Office, 1981, vol. 60, pp. 601–609.
44. Pearce, J. A. and Stern, R. J., Origin of back-arc basin magmas: trace element and isotope perspectives. *Geophys. Monogr*., 2006, **166**, 63–86.
45. Cabanis, B. and Lecolle, M., Le diagramme La/10-Y/15-Nb/8: un outil pour la discrimination des series volcaniques et la mise en evidence des processus de mélange et ou de contamination crustale. *Acad. Sci. Ser. II*, 1989, **309**, 2023–2029.
46. Srinivasan, K. N., Geology of Veligallu and Gadwal schist belts. *Rec. Geol. Surv. India*, 1990, **123**, 5.
47. Hoffmann, J. E., Munker, C., Polat, A., Rosing, M. T. and Schulz, T., The origin of decoupled Hf–Nd isotope compositions in Eoarchean rocks from southern West Greenland. *Geochim. Cosmochim. Acta*, 2011, **75**, 6610–6628.
48. Meffre, S., Aitchison, J. C. and Crawford, A. J., Geochemical evolution and tectonic significance of boninites and tholeiites from the Koh ophiolite, New Caledonia, Tectonics, 1996, **15**, 67–83.
49. Pearce, J. A., Geochemical fingerprinting of oceanic basalts with applications to ophiolite classification and the search for Archean oceanic crust. *Lithos*, 2008, **100**, 14–48.
50. Metcalf, R. V. and Shervais, J. W., Suprasubudction-zone ophiolites: is there really an opiolite conundrum? In *Ophiolites, Arcs, and Batholiths: A Tribute to Cliff Hopson* (eds Wright, J. E. and Shervais, J. W.), Geological Society of American Special Paper, 2008, vol. 438, pp. 191–222.
51. Rollinson, H. R., *Using Geochemical Data: Evaluation, Presentation, Interpretation*, John Wiley, New York, 1993, p. 351.
52. Gurenko, A. A. and Chaussidon, M., Enriched and depleted primitive melts in olivine from Icelandic tholeiites: origin by continuous melting of a single mantle column. *Geochim. Cosmochim. Acta*, 1995, **59**, 2905–2917.
53. McKenzie, D. and O'Nions, R. K., Partial melt distributions from inversion of rare earth element concentrations. *J. Petrol.*, 1991, **32**, 1021–1091.
54. Shaw, D. M., Continuous (dynamic) melting theory revisited. *Can. Mineral*., 2000, **38**, 1041–1063.
55. Vijay Kumar, K., Reddy, M. N. and Leelanandam, C., Dynamic melting of the Precambrian mantle: evidence from the rare earth elements of the amphibolites from the Nellore–Khamman schist belt, South India. *Contrib. Mineral. Petrol.*, 2006, **152**, 243–256.

ACKNOWLEDGEMENTS. This line of work was initiated by Dr C. Manikyamba under a DST-New Delhi sponsored project. I thank CSIR, New Delhi for Senior Research Fellowship and Drs D. V. Subba Rao, C. Manikyamba and M. Ram Mohan for their constant encouragement and discussions in the field. All analyses were performed at NGRI Geochemistry Laboratory, Hyderabad. I also thank Drs V. Balaram and A. Keshav Krishna for providing the ICP-MS and XRF analytical facility respectively and P. K. Prachiti and K. Raju for their assistance in the wet chemistry laboratory. I am grateful to Prof. Mrinal Sen, Director, NGRI, for permission to publish this work.

Received 9 December 2011; re-revised accepted 8 January 2013